

# Toward Improved Estimation of the Dynamic Topography and Ocean Circulation in the High Latitude and Arctic Ocean: The Importance of GOCE

J. A. Johannessen · R. P. Raj · J. E. Ø. Nilsen · T. Pripp ·  
P. Knudsen · F. Counillon · D. Stammer · L. Bertino ·  
O. B. Andersen · N. Serra · N. Koldunov

Received: 22 March 2013 / Accepted: 26 November 2013 / Published online: 23 January 2014  
© The Author(s) 2014. This article is published with open access at Springerlink.com

**Abstract** The Arctic plays a fundamental role in the climate system and shows significant sensitivity to anthropogenic climate forcing and the ongoing climate change. Accelerated changes in the Arctic are already observed, including elevated air and ocean temperatures, declines of the summer sea ice extent and sea ice thickness influencing the albedo and CO<sub>2</sub> exchange, melting of the Greenland Ice Sheet and increased thawing of surrounding permafrost regions. In turn, the hydrological cycle in the high latitude and Arctic is expected to undergo changes although to date it is challenging to accurately quantify this. Moreover, changes in the temperature and salinity of surface waters in the Arctic Ocean and Nordic Seas may also influence the flow of dense water through the Denmark Strait, which are found to be a precursor for changes in the Atlantic meridional overturning circulation with a lead time of around 10 years (Hawkins and Sutton in *Geophys Res Lett* 35:L11603, 2008). Evidently changes in the Arctic and surrounding seas have far reaching influences on regional and global environment and climate variability, thus emphasizing the need for advanced quantitative understanding of the ocean circulation and transport variability in the high latitude and Arctic Ocean. In this respect, this study combines in situ hydrographical data, surface drifter data and direct current meter measurements, with coupled sea ice–ocean models, radar altimeter data and the latest GOCE-based geoid in order to estimate and assess the quality, usefulness and validity of the new GOCE-derived mean dynamic topography for studies of the ocean circulation and transport estimates in the Nordic Seas and Arctic Ocean.

---

J. A. Johannessen (✉) · R. P. Raj · J. E. Ø. Nilsen · T. Pripp · F. Counillon · L. Bertino  
Nansen Environmental and Remote Sensing Center, Bergen, Norway  
e-mail: Johnny.Johannessen@nersc.no

P. Knudsen · O. B. Andersen  
National Space Institute, Technical University of Denmark, Lyngby, Denmark

D. Stammer · N. Serra · N. Koldunov  
Center für Erdsystemforschung und Nachhaltigkeit (CEN), University of Hamburg, Hamburg,  
Germany

**Keywords** Oceanography in the Arctic Ocean and surrounding seas · Mean dynamic topography · Surface current · GOCE satellite

## 1 Introduction

Changes in the dynamic topography and ocean circulation between the northern Atlantic Ocean and the Arctic Ocean result from variations in the atmospheric forcing field and convective overturning combined with changes in freshwater runoff and their pathways, mean sea level, sea ice deformation and water mass transformation. The ocean circulation in this region has been subject to investigations since Helland-Hansen and Nansen (1909). In general, it can be characterized by four regional circulation regimes and cross-regional exchanges and volume transports, namely the Northeast Atlantic, the Labrador Sea and Canadian archipelago, the Nordic and Barents Seas and the Arctic Ocean, as illustrated in Fig. 1.

Accurate knowledge of the ocean transport variability together with understanding of the water mass transformations within and across these regions is highly needed to quantify changes in the overturning circulation with acceptable uncertainty. The Atlantic meridional overturning circulation is, among other factors, influenced by: variations in the upper ocean and sea ice interaction; ice sheet mass changes and their effect on the regional sea-level change; changes in freshwater fluxes and pathways; and variability in the large-scale atmospheric pressure field. For instance, changes in the pathways of the freshwater from the Eurasian runoff forced by shifts in the Arctic Oscillation can lead to increased trapping of freshwater in the Arctic Ocean as presented by Morison et al. (2012) that, in turn, may alter the thermohaline circulation in the sub-Arctic Seas.

Using a new combination of the ice cloud and land elevation satellite (ICESat) laser altimeter and the gravity recovery and climate experiment (GRACE) satellites, along with traditional hydrography, Morison et al. (2012) were able to show that the dominant freshwater changes from 2005 to 2008 were an increase in surface freshwater in the Canada basin balanced by a decrease in the Eurasian basin. These changes were due to a cyclonic (anticlockwise) shift in the ocean pathway of the Eurasian runoff forced by strengthening of the west-to-east Northern Hemisphere atmospheric circulation corresponding to a strengthening of the Arctic Oscillation index. These findings are confirmed in recent results presented by McPhee (2013) and Koldunov et al. (2013). In addition, the regional sea level jointly obtained from tide gauges and ERS-1, 2 and Envisat altimeter satellites together with the gravity field and ocean dynamic topography observations from GRACE and GOCE have also recently allowed new innovative studies of the climate-critical mass changes and freshwater flux variations in the high latitude and Arctic Ocean (e.g., Cheng et al. 2013; Prandi et al. 2012; Henry et al. 2012; Knudsen et al. 2011).

In this paper, a new GOCE-based geoid and mean dynamic topography (MDT) for the high latitude and Arctic Ocean is obtained, assessed and compared to independent steric height observations and state-of-the-art MDTs. Furthermore, comparisons of surface velocity and transport in the Nordic Seas, based on the combination of GOCE gradiometer gravity estimates and in situ hydrographic data, are done with estimates from several forced coupled sea ice–ocean models, ocean surface drifter data and direct measurements. The new findings and results are presented according to the ocean dynamic topography in Sect. 2, ocean surface circulation in Sect. 3 and volume transport in Sect. 4. A summary follows in Sect. 5.

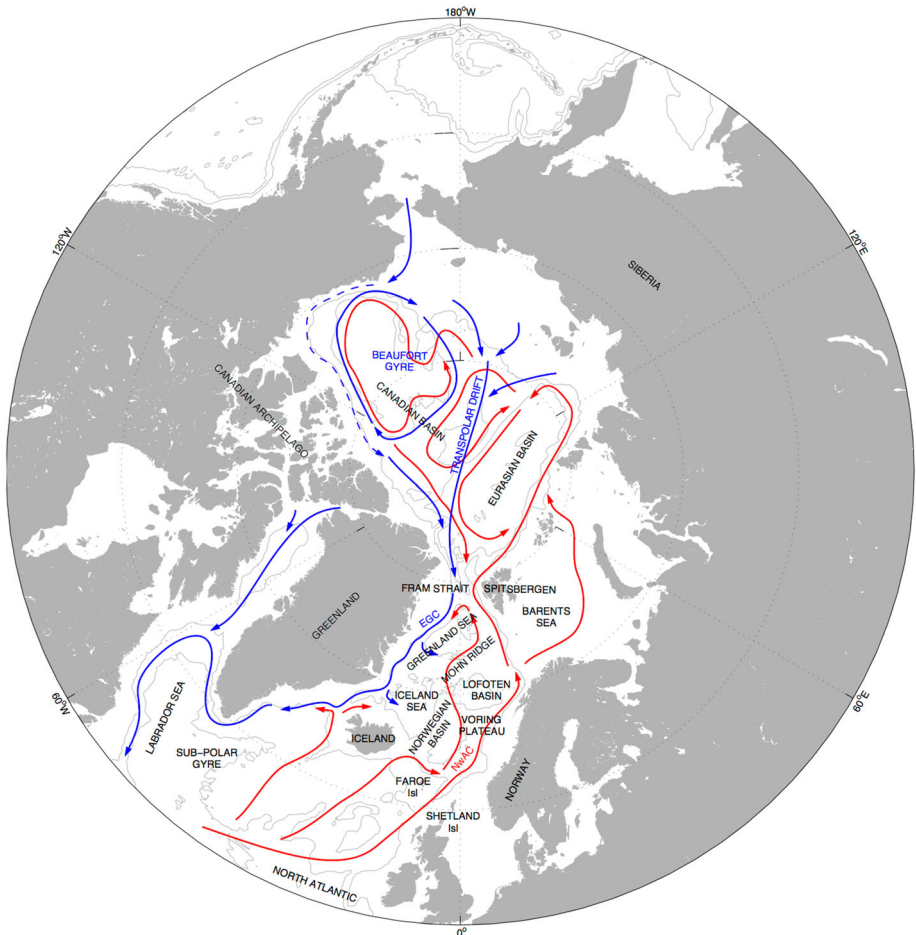


**Fig. 1** General circulation of the Arctic Ocean, Nordic Seas, and North Atlantic. Bottom contours are 1000 and 3000 m outlining the shelves and basins. *Red arrows* represent Atlantic Waters, which reside in the surface in the Nordic Seas and submerged in the Arctic Ocean. *Blue arrows* represent Polar Water, residing in the surface. The Norwegian Sea comprises the Norwegian Basin, while Lofoten Basin, while the Nordic Seas are the Norwegian, Iceland and Greenland Seas. Circulation patterns based on AMAP (1998) and Furevik and Nilsen (2005)

## 2 Ocean Dynamic Topography

Measurements of the sea surface height have been routinely obtained from satellite altimeter missions, such as the TOPEX/POSEIDON (Fu et al. 2001; Shum et al. 2010), in the last 20 years. Today, the annual mean sea surface (MSS) height derived from altimetry is known with millimeter accuracy (e.g., Cazenave et al. 2009) in the open ocean. In addition, knowledge of the marine geoid has drastically improved thanks to satellite gravity measurements from the NASA GRACE (Maximenko et al. 2009) and ESA GOCE (Johannessen et al. 2003; Bingham et al. 2011; Knudsen et al. 2011) missions in the last decade. In turn, the MDT, which is simply the difference between the mean sea surface height (MSS) and the geoid (G) (both referenced to the same ellipsoid as illustrated in

Fig. 2), can now be determined with new and unprecedented accuracy around  $\approx 3$  cm at 100 km spatial resolution (Bruinsma et al. 2013). In comparison to the use of the reference geoid obtained from the Earth Gravitational Model 2008 (EGM2008), this yields a factor 2 improvement in the MDT at this spatial resolution. However, this accuracy is not necessarily applicable to the Arctic Ocean and the neighboring sub-Arctic seas due to the presence of sea ice, lack of Jason altimeter coverage and shorter dominant spatial scales.

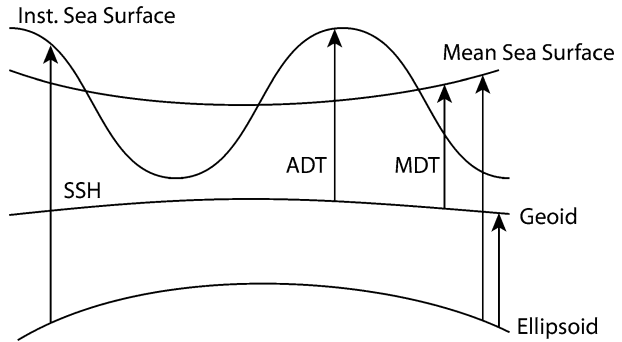
The GOCE high-level processing facility (HPF) delivers the level-2 global gravity model from which geoid heights can be determined (Koop et al. 2007; Bingham et al. 2011). Based on 12 months of GOCE data acquired in the time interval November 01, 2009 to April 14, 2011, three versions of GOCE gravity model are made available: the direct (DIR) approach; the spacewise (SPW) approach; and the timewise (TW) approach. More details of these gravity field models can be obtained from Bruinsma et al. (2010) and Pail et al. (2011). In addition, so-called combination models such as the EIGEN-6C (Förste et al. 2011) that combines the GOCE data with terrestrial data have been developed. In this paper, we apply the EIGEN-6C gravity model for the computation of the MDT. The corresponding geoid is determined in the mean-tide system and relative to a Topex-ellipsoid. This ensures consistency with the Technical University of Denmark (TUD) MSS data set referenced to the time period 1993–2009 (Andersen and Knudsen 2009). Subsequent to subtracting the geoid from the MSS, filtering was carried out eliminating the short wavelength geoid signals, in order to obtain a useful estimate of the MDT. This filtering was carried out using a 80-km Gaussian filter to preserve the upper bound of the mesoscale features in the study area. (Note that Knudsen et al. (2011) applied a 140-km Gaussian filter to determine the global ocean MDT.) In the forthcoming, we refer to this as the GOCE-based geoid and MDT.

Isolines of constant MDT (MSS-G) are usually considered as a stream function for the large-scale ocean surface circulation, which the surface geostrophic currents are directed along. In the Northern Hemisphere (Southern Hemisphere), the flow is clockwise (anti-clockwise) around the topographic high. The magnitude of the global spatial MDT variations is around 2–3 meters, which is about two orders of magnitude smaller than the global spatial changes in the marine geoid and the MSS. This makes the computation of the MDT and the handling of errors challenging as it is easy to fail to exploit all of the details in the geoid and the MSS when calculating the MDT because of the need to obtain a smooth solution. Herein, the separation of the MDT from the MSS and the geoid is carried out in the space domain, where the MSS is usually represented using processing tools that are available at the dedicated ESA GOCE User Toolbox (GUT); see Web site <http://earth.esa.int/gut/>.

The GOCE-based MDT shape and spatial pattern representing the mean from 1993 to 2009 for the North Atlantic, Nordic Seas and the Arctic Ocean is shown in Fig. 3. The total MDT elevation range from the high in the Arctic Ocean to the low in the subpolar gyre in the North Atlantic reaches about 0.9 m. The regional shape of the MDT with the orientation of the dominant slopes in the different sub-domains reveals the presence of the main circulation pathways in: (1) the subpolar gyre south of Greenland; (2) the inflow of Atlantic Water, respectively, between Iceland and the Faroe Islands and between the Faroe and Shetland Islands; (3) the continuous northward flowing Atlantic Water toward the Arctic Ocean; (4) the southward flowing East Greenland Current (EGC); (5) the Beaufort Gyre; and (6) the transpolar drift in the Arctic Ocean.

The MDT in the Arctic Ocean may display some characteristic features that are caused by problems in the data coverage. Both the GOCE data and the altimeter data do not cover the Arctic Ocean entirely, so within 300–400 km from the pole, the data coverage is

**Fig. 2** Schematic illustration of the relationship between the absolute and mean dynamic topography (ADT and MDT), the mean sea surface and the geoid referenced to the same ellipsoid. Note the difference between the instantaneous sea surface and the MDT



insufficient to calculate a reliable MDT. Also, the presence of sea ice may hamper the computation of the MSS and hence the MDT. Though care is taken to avoid erroneous data some of the data that have been used to calculate the MSS may represent the top of the sea ice floes rather than the sea surface. In particular, off the coasts of the Canadian Archipelago and northern Greenland the high values of the GOCE MDT may be caused by the influence of the permanent and thick sea ice cover.

The Arctic Ocean displays an elevation change reaching up to about 0.45 m associated with the high in the Beaufort Gyre, and with the corresponding dominant orientation of the slope mostly aligned from Siberia to the northern shores of Greenland. According to Steele and Ermold (2007), the dynamic height in the Arctic Ocean is predominantly influenced by salinity. In the Nordic Seas, the general shape of the MDT favors the cyclonic circulation pattern displaying steepest MDT slopes of 0.4 m/100 km between the Faroe and Shetland Islands, along the northwest coast of Norway and in the northern part of the EGC. In comparison, the slope across the Gulf Stream reaches 1 m/100 km. This spatial pattern in the MDT agrees well with the spatial pattern in the mean steric height derived from hydrographic data (Nilsen et al. 2008) for the period 1950–2010, respectively, referenced to 500, 1,000 and 1,500 m as shown in Figs. 4 and 5b.

The steric height calculation is done according to Siegismund et al. (2007), where the steric height is referenced to a constant density  $\rho_0$  from salinity of 35 and temperature of 0 °C. More information on the concept and application of the steric height is given by Tomczak and Godfrey (2003). The difference in these height fields primarily reveals the effect of the vertical distribution of temperature and salinity in the upper 1500 m, predominantly influenced by the advection and spreading of the Atlantic Water. Apart from the changes occurring in the Lofoten Basin, the overall structure remains largely unchanged when the density structures from 1,000 to 1,500 m are included. This suggests that the baroclinic circulation in the Nordic Seas is driven by the temperature and salinity structures of the Atlantic Water in the upper 1,000 m.

In the Nordic Seas, the total range in the MDT derived from the combined GOCE and altimetry data is around 0.50–0.55 m as seen in Fig. 5a. In comparison, the range of the mean steric height of 0.30 m (Fig. 5b) suggests that there might be a significant contribution to the MDT pattern from the large-scale atmospheric pressure field and the deep barotropic currents in some of the sub-basins. Siegismund et al. (2007) moreover concluded that the seasonal cycle of the steric height (for the period 1950–1999) is predominantly associated with the temperature variations in agreement with previous studies on global scale (e.g., Gill and Niiler 1973; Stammer 1997; Mork and Skagseth 2005). By subtracting the hydrographic-based steric height associated with the baroclinic structure in

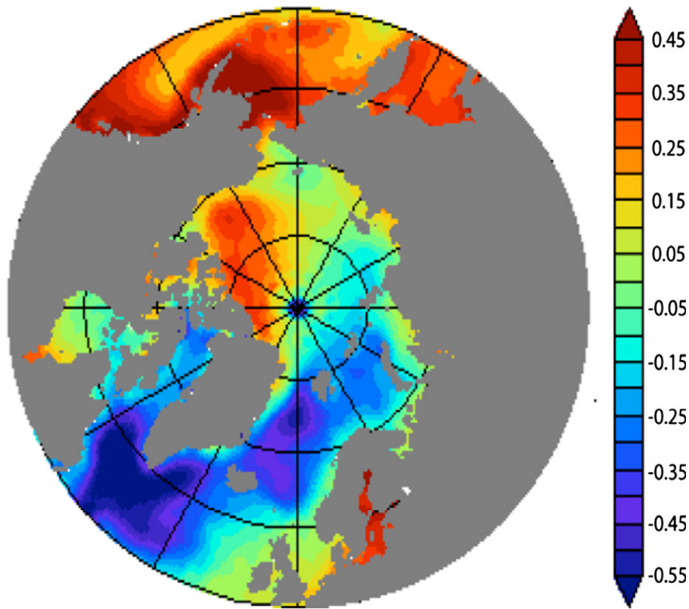


**Fig. 3** Mean dynamic topography (MDT) derived from the GOCE gradiometer data (release 3) and altimetry (from 1993 to 2009) with a spatial resolution of about 100 km. Color bar is in units of meter. The structures in the North Pacific are not investigated further in this paper. Note that the GOCE data (release 4) available since March 2013 are more accurate due to more than a doubling in the amount of data

the water masses from the GOCE-based MDT, an estimate of the barotropic contribution to the MDT is derived as shown in Fig. 5c. The barotropic contribution contains distinct elevation changes of about 10 cm having pattern consistent with the known barotropic cyclonic circulations in the Greenland Sea, the Lofoten Basin and in the Norwegian Sea (Nøst and Isachsen 2003). Evidence of this cyclonic barotropic circulation in the Norwegian Sea has also been observed from Argo floats in the intermediate waters below the Norwegian Atlantic Current (Sjøiland et al. 2008). In summary, the assessment of the GOCE-derived MDT for the Nordic Seas and the Arctic Ocean is promising.

In view of the promising GOCE-based results presented above, they are also providing a new opportunity for inter-comparison and validation of coupled sea ice–ocean models and reanalyses fields. As specified in Table 1, the three models used in this inter-comparison study include the regional setup of the ATL (MITgcm) model (Serra et al. 2010); the MICOM model (Sandø et al. 2012); and the HYCOM model (Bleck 2002; Sakov et al. 2012). The models are either forced by the 6 hourly NCEP reanalysis field (ATL and MICOM) or the ERA Interim field (HYCOM).

Ignoring the offset in the mean MDT, the three coupled sea ice–ocean models in general reproduce comparable overall spatial structure of the MDT in the Arctic Ocean, the Nordic Seas and the North Atlantic, notably the high in the Beaufort Gyre and the depressions in the Nordic Seas and the subpolar gyre (Fig. 6). The model highs in the Beaufort Gyre are circular and located toward the deep Canadian Basin with decreasing values toward the Eurasian Basin, providing an elevation difference of 0.5–0.6 m. The MICOM-field, however, has a gyre that extends into the Eurasian Basin. In comparison, the GOCE-based elevated feature in the Beaufort Sea is shifted more toward the Canadian Archipelago, while the total elevation

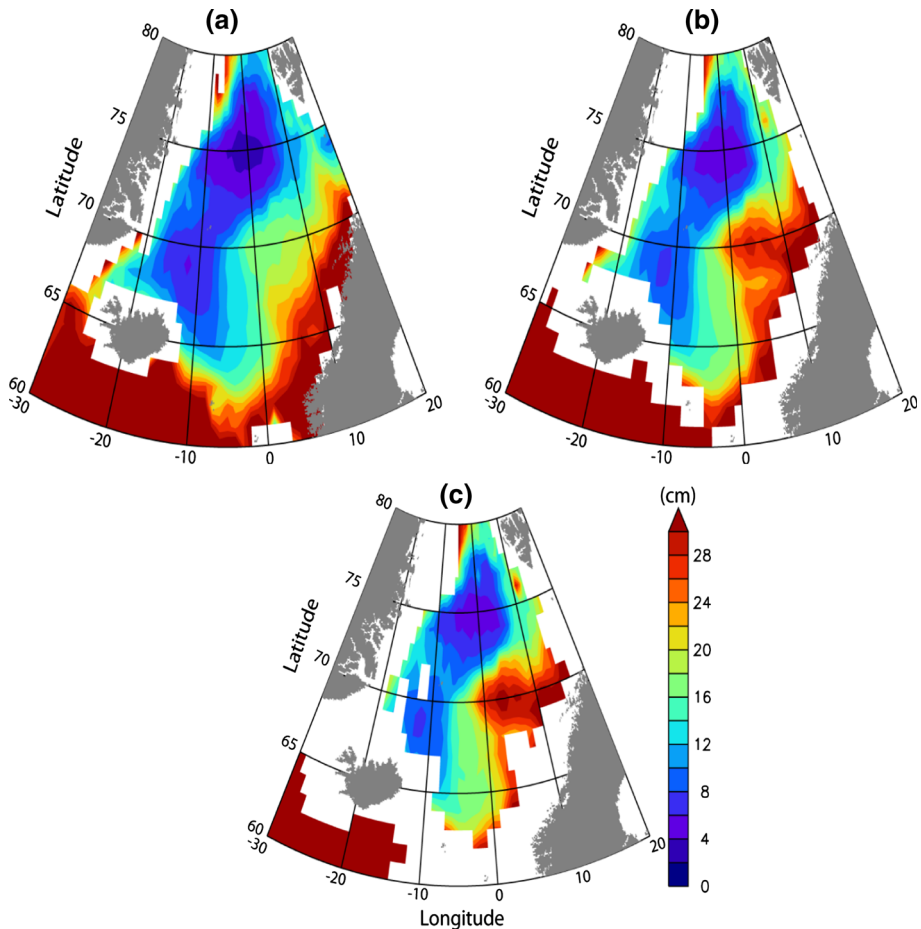


**Fig. 4** Observed mean steric height for the period 1950–2008 for the reference depths **a** 500 m, **b** 1,000 m and **c** 1,500 m. The color-scale increment is in cm

difference remains the same. This shift in location is in agreement with the recent findings by Kwok and Morison (2011) and Morison et al. (2012). Overall, the MDT patterns in the model fields for the Arctic Ocean are in reasonably good agreement with the GOCE-based MDT map.

In the central domain of the Norwegian-Greenland Seas, the suppression of the MDT in the three models corresponding to the large-scale cyclonic circulation pattern with the northward flowing Norwegian-North Atlantic Current (NwAC) and the southward flowing EGC is consistent in location. On the other hand the magnitudes and spatial structures of the suppression differ between the models as well as in comparison with the GOCE-based MDT pattern. The largest suppression is found in the ATL model with a deviation from the average of  $-0.6$  m in the northern Greenland Sea being almost twice as large as in the GOCE-based MDT in the same area. Similar tendencies are seen in the subpolar gyre, although the difference in the minima between the ATL model and the GOCE-based MDT now is reduced by a factor of 2.

The most prominent discrepancies are the mismatch in the MDT along the Canadian Archipelago and northern Greenland coast, and the models lack of higher elevations associated with the spread of AW in the Norwegian Sea, notably around the Vøring Plateau. The former

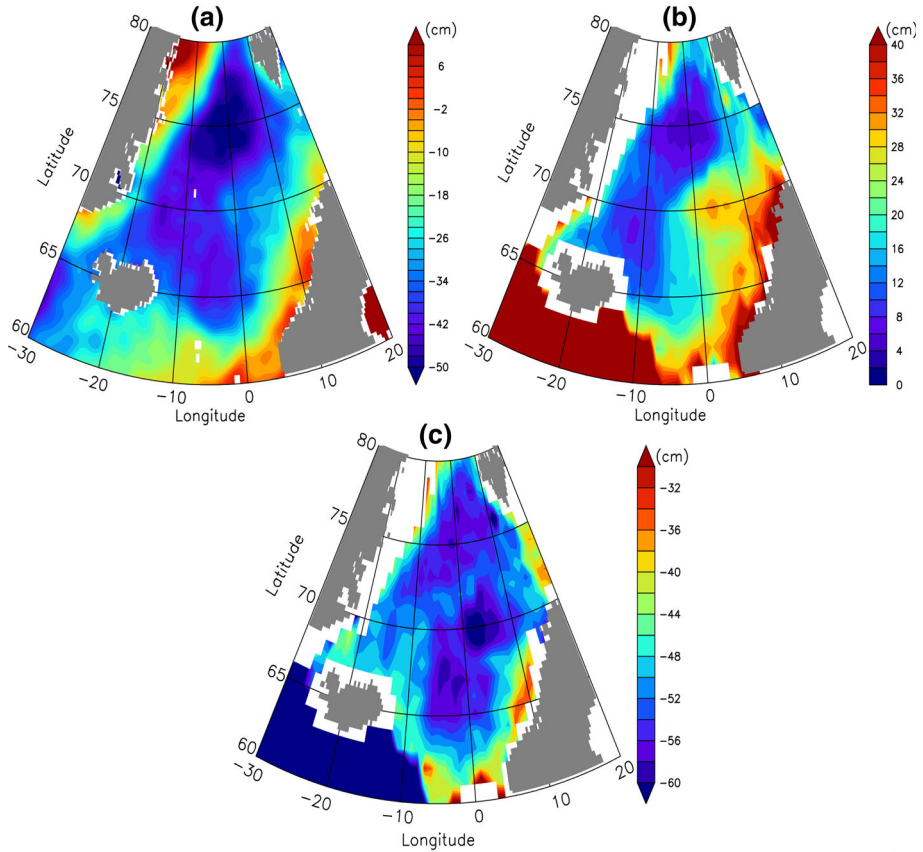


**Fig. 5** **a** MDT derived from combined GOCE and altimetry, **b** steric height derived from the in situ hydrographic database where the *white* areas in the 1,500 m reference steric height (see Fig. 4) are filled with steric height values representing every 100 m from 1,400 to 500 m, and **c** difference between (a) and (b). The color bars represent the height contours in unit of cm. Note the different *color* ranges

might be related to the presence of thicker multiyear sea ice that could influence the estimation of the MSS and thus the GOCE-based MDT. Kwok and Morrison (2011) did not reveal this particular high in the MDT confined to the coastal region from IceSAT data. The latter is related to the topographic steering of the baroclinic western branch of the NwAC (Nilsen and Nilsen 2007), as well as eddy transport of buoyant waters from the slope branch of the NwAC into the Lofoten Basin (Rossby et al. 2009), which are both challenging to model. Furthermore, although totally lacking the broadness of the NwAC, the ATL model is the only model with the doming of the densest waters of the Nordic Seas placed in the correct basin, the Greenland Basin.

These differences in magnitude and spatial structure of the model and GOCE-based MDTs imply different strengths and orientations of the slopes in the MDT. In turn, the mean surface geostrophic currents are expected to have discrepancies that subsequently will lead to differences in the estimation of the associated transport of water masses. This is further assessed in the next sections.

**Table 1** Characterization of the three coupled sea ice–ocean models used for inter-comparison to the GOCE-derived MDT and mean surface geostrophic current

Model run	Region	Spatial resolution	Period	Vertical grid, # of layers, forcing
ATL12	Atlantic Ocean north of 33°S including the Nordic Seas and the Arctic Ocean. Uses ETOPO 2-min resolution bathymetry	~ 8 km	1948–2009 Hindcast	z-coordinates, 50 levels, NCEP—6 h
MICOM	North of 30°S with Nordic Seas and Arctic Ocean included. Uses ETOPO 1 5-min resolution bathymetry	~ 15 km	1948–2007 Hindcast	Isopycnal, 35 layers, NCEP—6 h
HYCOM	High latitude- Arctic Ocean. Uses GEBCO 1-min resolution bathymetry	~ 12–16 km	1993–2010 Hindcast	Hybrid coordinates, 28 layers, ERA Interim—6 h

*ETOPO 2-min* Earth's relief data set with a grid size of 2' by 2', from NOAA Geophysical Data Center  
NCEP relates to US National Centers for Environmental Prediction

*GEBCO 1-min* Earth's relief data set with a grid size of 1' by 1', from UNESCO and IOC  
ERA relates to European Center for Medium-Range Weather Forecasting Reanalyses

### 3 Surface Circulation

With access to the new GOCE-based MDT with unprecedented accuracy, the uncertainties in mean ocean circulation and transport estimation are expected to improve. The mean surface geostrophic velocities are computed from the MDT, under the assumption of geostrophic balance;

$$u_s = \frac{-g}{f} \cdot \frac{\partial MDT}{\partial y} \quad (1)$$

$$v_s = \frac{g}{f} \cdot \frac{\partial MDT}{\partial x} \quad (2)$$

where  $u_s$  and  $v_s$  are components of the surface geostrophic velocity,  $g$  is the acceleration due to gravity,  $f$  is the Coriolis parameter, and  $x$  and  $y$  are the longitudinal and latitudinal coordinates. The corresponding surface geostrophic current derived from the GOCE MDT for the Nordic Seas over the period 1993–2009 is shown in Fig. 7 and compared to the independently derived CNES\_CLS09 MDT Rio et al. 2011 and Maximenko et al. 2009 (which both are using a GRACE-based geoid model together with in situ Argo floats and surface drifter data integrated over the 17-year period from 1992 to 2009), as well as the climatological mean surface velocities (predominantly based on drifters in the Nordic Seas from 1991 to 2010) from the surface drifter data ([http://www.aoml.noaa.gov/phod/dac/drifter\\_climatology.html](http://www.aoml.noaa.gov/phod/dac/drifter_climatology.html)).

The large-scale cyclonic surface circulation regime is well-reproduced in all three fields. However, while the strongest mean surface currents of the inflowing Atlantic Water to the Norwegian Sea reaching nearly 0.20 m/s are derived from the GOCE MDT, the inflow in the other two surface current fields is clearly weaker with maximum speed not much more than 0.10 m/s. Moreover, it is only the GOCE-based surface geostrophic current that reveals distinct

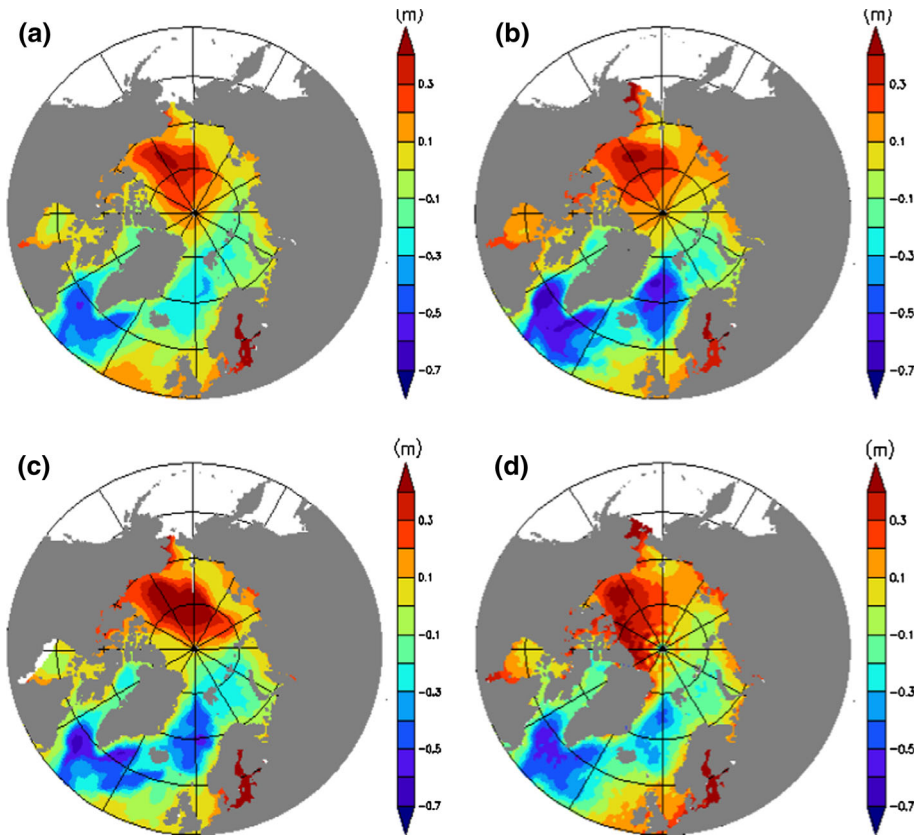


**Fig. 6** MDT fields referenced to the full-region average: **a** the HYCOM MDT (free run) from 1993 to 2010, **b** the ATL from 1993 to 2009, **c** the MICOM from 1993 to 2007, and **d** the GOCE-based MDT from 1993 to 2009. The *color bars* are in meters. All the fields are interpolated to a  $0.25^\circ$  resolution grid

expressions of cyclonic circulation in the Greenland Basin, Norwegian Basin and Iceland Sea, as well as the broadening of the NwAC over the Vøring Plateau and in the Lofoten Basin, i.e., signs of a proper western (baroclinic) branch of the northward flowing Atlantic Water. From this inter-comparison and assessment, it is therefore evident that the GOCE-based geoid provides a reliable representation of the MDT and mean ocean surface circulation in the Nordic Seas. Evidently, this is further supported by the mean surface circulation pattern derived from the climatology of the surface drifter data as shown in Fig. 7d.

A comparison of the speed of the GOCE-based mean surface geostrophic currents and corresponding model-based currents for the Nordic Seas is shown in Fig. 8. In general, it must be emphasized that the finer spatial model resolution versus GOCE may favor stronger simulated surface speeds. All models indicate intensified currents at the inflows from the northeast Atlantic Ocean, and in the boundary (slope) currents of the Nordic Seas. The ATL model shows a strengthened component of internal circulation in the Nordic Seas, by very strong currents along all the margins. Regarding the currents over the mid-ocean ridges and other internal topographic features, it is only the MICOM run that shows signs of reproducing the level of intensification shown in the GOCE-based speeds, however only at one location, the Mohn Ridge (as also noticed in Fig. 7d).

For a more detailed study of the seasonal variability induced by the altimetric observations, the surface slopes and meridional velocities across 75°N are presented in Fig. 9 together with the model-derived fields. The seasonal mean meridional velocities are estimated by replacing MDT in Eq. (2) with absolute dynamic topography (ADT). Note that ADT is determined as the sum of MDT and monthly mean sea-level anomaly (SLA) data. The new high-resolution SLA data (obtained from the French CLS-led Sea Level Climate Change Initiative project funded by ESA) are referenced to the time period 1993–2009 and hence consistent with the DTU MSS data used in the calculation of GOCE MDT.

The main expected features of the flow toward and from the Fram Strait is revealed by the mean velocities: the two branch northward flowing West Spitsbergen Current (WSC) around 8° and 15°E; the strong southbound EGC at 10°W; and some minor, possibly cyclonic, circulation features around 0°E, likely related to circulation in the Boreas Basin. Seasonal differences are most pronounced in the WSC. Both branches are strongest in wintertime, with a near doubling of the easternmost branch, which is due to the general (wind driven) intensification of the circulation in the region. This is consistent with velocity retrievals and transport estimates reported by Mork and Skagseth (2005). The western frontal branch stays relatively strong also during the rest of the year, likely due to the summertime spread of buoyant surface water from the coast to the front (as seen further south in the NwAC; Nilsen and Falck 2006), maintaining a steep frontal surface slope.

In comparison, the model-based MDT slopes along 75°N and the corresponding meridional geostrophic velocities across the same latitude consistently reveal that the ATL model has the steepest surface slopes and hence the strongest flow field for both the northward flowing NwAC as well as the southward flowing EGC. Moreover, it is only the ATL model that reproduces the double peak in the WSC current in agreement with the mean and seasonal observation-based findings.

#### 4 Volume Transport

By combining the GOCE-derived MDT and altimetric sea-level anomalies (SLA) with the comprehensive hydrographic database, an estimate of the mean and variable transport of Atlantic Water entering the Nordic seas is obtained for the period 1993–2011 at a spatial resolution of 100 km. Using 44 CTD-sections in the Faroe north section normally taken to represent the Iceland-Faroe Ridge (IFR) inflow (Hansen et al. 2010), 84 CTD-sections for the Faroe–Shetland Channel (FSC) and 76 CTD-sections taken along the Svinøy section (see Fig. 8 for locations), the baroclinic velocity structures in the Atlantic Water defined by salinity values  $S > 35$  were estimated across these sections. Combined with the barotropic velocity values, the absolute velocities are then retrieved, and when these are multiplied by the area covered by the Atlantic Water, we obtain estimates of the corresponding volume transports of Atlantic Water across the 3 sections (see Table 2).

From the combination of GOCE, altimetry and hydrography, the mean inflows of Atlantic Water across the IFR and through the FSC are estimated to approximately 3.5 and 4.1 Sv, respectively ( $1 \text{ Sv} = 10^6 \text{ m}^3 \text{ s}^{-1}$ ). The former is in very good agreement with Hansen et al. (2010), but too low compared to Østerhus et al. (2005), while the latter is too high compared to Østerhus et al. (2005) and too low compared to Sandø et al. (2012). In comparison, the mean transport of the two branches of Atlantic Water crossing the Svinøy section, e.g., the Norwegian Atlantic Slope Current (NwASC) and the Norwegian Atlantic Front Current (NwAFC) is, respectively, 3.9 Sv and 3.0 Sv. The latter value is in acceptable agreement with previous transport estimates for the NwASC reported by Mork

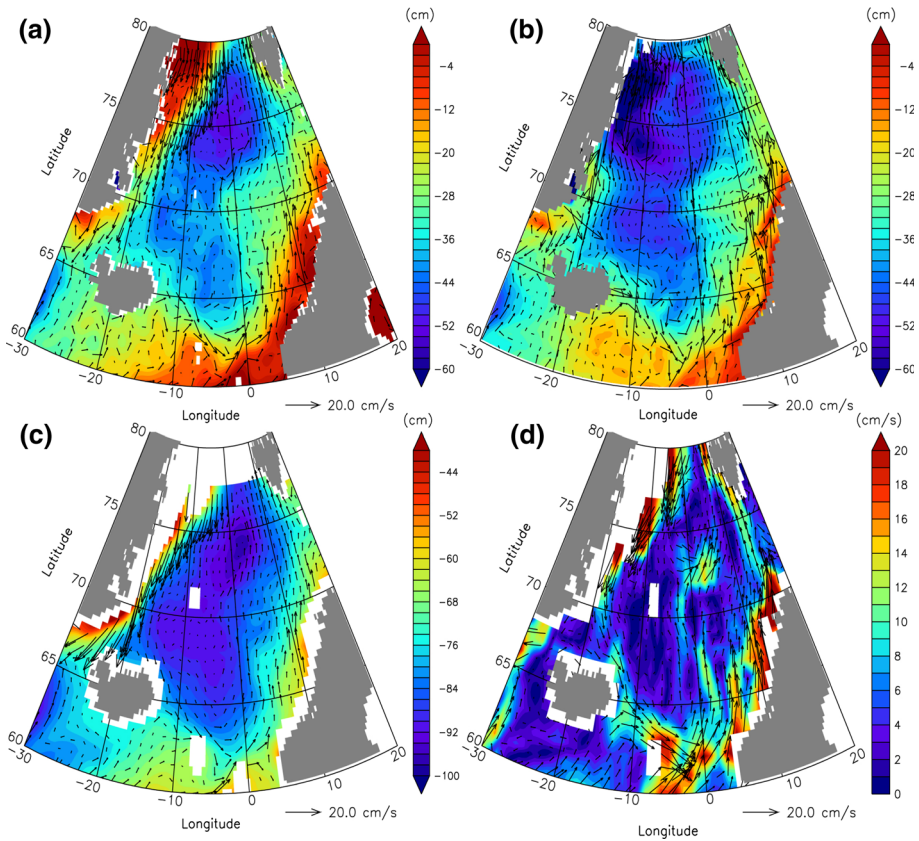


**Fig. 7** Mean surface geostrophic velocities shown by vectors superimposed on corresponding mean dynamic topography (MDT) derived from **a** GOCE, **b** CNES\_CLS09, **c** Maximenko et al. (2009), and **d** mean surface velocity vectors derived from the climatology of the global surface drifter data. Color scale indicates the MDT in cm for (a) to (c) and speed in cm/s for (d). Current-vector scale shown in the lower right corner

and Skagseth (2010); Orvik and Skagseth (2003, 2005); Skagseth et al. (2008); and Orvik et al. (2001) as documented in Table 2, taking into account the slight differences in the integration periods. On the other hand, the total combined GOCE-based and hydrographic transport estimates across the Svinøy section is about 35 % larger than other reported findings (e.g., 6.9 vs. 5.1 Sv).

In comparison, the mean (1993–2007) transports estimated from the three models across these sections show quite different values as noticed in Table 2. One explanation for this is partly related to the definition and choice of layers for the transport estimations. For instance, Sandø et al. (2012) defines the Atlantic Water (AW) as water in model layers above the pycnocline ( $\sigma_2 < 36.9 \text{ kg m}^{-3}$ ), which is representative of the interface between inflowing and outflowing waters throughout the integration. In contrast, Berx et al. (2013) simply uses  $T > 3 \text{ }^\circ\text{C}$  as definition for the AW in their calculation of the transport of AW across the IFR section. The best agreement between the model and the combined GOCE-based and hydrographic data is clearly obtained for the ATL simulation with transport estimates across the IFR and FSC of 3.5 and 4.2 Sv, respectively.

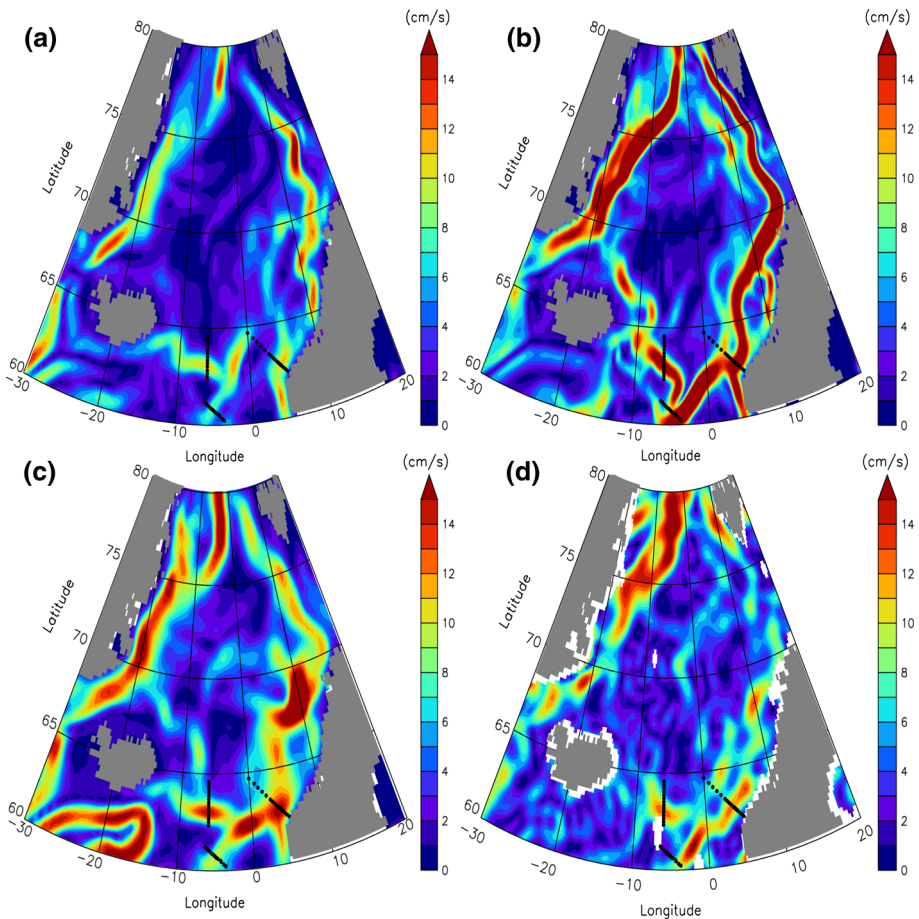


**Fig. 8** Inter-comparison of models and GOCE-based mean absolute surface geostrophic velocity from **a** the HYCOM model from 1993 to 2010, **b** the ATL model from 1993 to 2009, **c** the MICOM model from 1993 to 2007 and **d** GOCE. The color bars are in cm/s. The three black dotted lines mark the position of the Farøe north section, the Farøe–Shetland Channel section and the Svinøy section

For the Svinøy section, the comparison is, in general, less satisfactory. The HYCOM model clearly underestimates the observed transport of 5.1 Sv reported by Mork and Skagseth (2010) as well as the GOCE-based estimate of 6.9 Sv. This is mainly due to a mis-location of the NwAFC in the HYCOM simulation as seen in Fig. 8a. In contrast, the MICOM and ATL models, having comparable mean transport estimates in the range of 8.2–8.5 Sv overestimate both the GOCE-based estimate and the transport reported by Mork and Skagseth (2010). Overall, this large spread in mean transport estimates implies significant differences in the mean northward advection of heat and salt to the Nordic Seas and Arctic Ocean. This, in turn, affects both the evaporation–precipitation fluxes and convective overturning in the Norwegian and Greenland Seas. Further studies are needed to investigate the accuracies of these transport estimates.

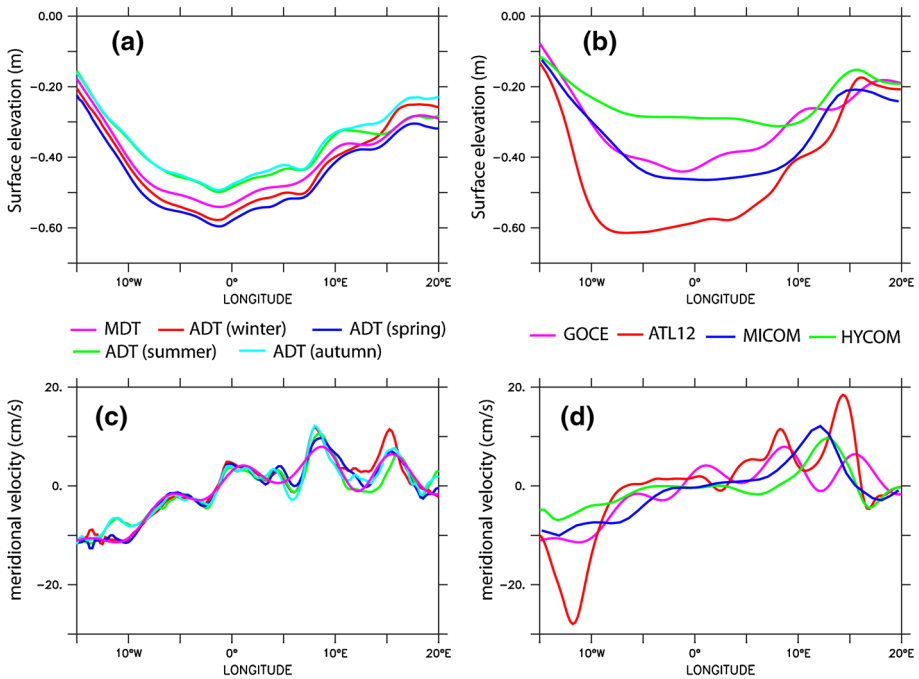


**Fig. 9** Climatologies of (a, b) dynamic topography across 75°N and (c, d) corresponding meridional absolute geostrophic velocities: (a, c) seasonal climatologies from combined GOCE-based MDT and altimetry and (b, d) comparison of GOCE-based MDT with MDT from ATL12, MICOM and HYCOM. Note that in (b), each MDT is referenced to its full-region average as defined in Fig. 6

Taking benefit of the temporal variability observed in the SLA and hydrographic data, the mean and seasonal cycle in the transport of the inflowing Atlantic Water for the period 1993–2009 can also be estimated and inter-compared as shown in Fig. 10.

On average, the NwASC contains approximately 57 % (or 3.9 Sv) of the total mean volume transport across the Svinøy section of about 6.9 Sv. The mean seasonal variability reveals a pattern with largest transports (9.3 Sv) in winter being 70 % larger than the summer transport minimum (5.4 Sv). Moreover, the mean seasonal NwASC transport always exceeds the mean seasonal NwAFC transport, while the latter displays a narrower range of seasonal variability in the volume transport. This suggests that the seasonal changes of the transport across the Svinøy section are predominantly controlled by seasonal changes in the transport of the NwASC.

The partitioning of these total transport estimates (both in the mean and seasonal signals) into the respective barotropic and baroclinic components is shown in Fig. 10b, c and reveals distinct differences. While the transport in the NwASC is dominated by the barotropic flow as expected along the shelf break at the Svinøy section, the transport of the NwAFC, in contrast, is clearly larger in the baroclinic component with the exception of the autumn period.

These GOCE-based estimates together with high-quality in situ hydrographic data are providing new and promising abilities to examine the seasonal transport variability (total as well as barotropic and baroclinic components) across key-selected sections. As such, it is also providing an important tool for validations of model circulation and transports between the northeast Atlantic Ocean and the Nordic Seas and Arctic Ocean.

**Table 2** Comparison of volume transport estimates from combined GOCE, altimetry and in situ hydrography to previous studies as well as estimates from simulation models for the Island-Faroe Ridge (IFR), Faroe–Shetland Channel (FSC), NwAFC, NwASC in the Svinøy Section and the total Svinøy Section

Source	Data	Period	IFR [Sv]	FSC [Sv]	Svinøy [Sv]		
					NwAFC	NwASC	Total
The current study	GOCE + Altim. + hydr.	1993–2011	3.5	4.1	3.0	3.9	6.9
Mork and Skagseth (2010)	Altim. + hydr.	1993–2009			1.7	3.4	5.1
Skagseth et al. (2008)	Current meter	1995–2006				4.3	
Orvik and Skagseth (2005)	Curr. meters	1995–1999				4.2	
Orvik and Skagseth (2003)	Curr. meters	1998–2000				4.4	
Orvik et al. (2001)	Curr. meters + ADCP + hydr.	1995–1999			3.4	4.2	7.6
Berx et al. (2013)	Altm. + ADCP + hydro	1995–2009	3.5				
Østerhus et al. (2005)	Bottom ADCP + hydr.	1999–2001	3.8	3.8			
Hansen et al. (2010)	Bottom ADCP + hydr.	1997–2008	3.5				
Sandø et al. (2012)	MICOM model	1994–2007	4.7*	4.7			
The current study	HYCOM model	1993–2007	1.8	1.5	2.0	0.6	2.6
The current study	MICOM model	1993–2007	3.5	6.9	3.5	5.0	8.5
The current study	ATL model	1993–2007	3.5	4.2	3.5	4.7	8.2

\* Only from 1997 to 2007

## 5 Summary

In combination with in situ hydrographical data, surface drifters and current meter measurements, coupled sea ice—ocean models and the latest GOCE-derived geoid and MDT (Pail et al. 2011), the paper has investigated the quality, usefulness and validity of the new GOCE data for studies of the ocean circulation and transports in the Nordic Seas and Arctic Ocean. Using the GOCE data from release number 3 (based on 12 months of GOCE data in the time interval 1 November 2009 to 2014 April 2011), the gravity model from the direct approach yields the computation of the GOCE-based geoid, and jointly with the DTU10 MSS data (based on the integration over the period 1993–2011, Knudsen et al. 2011), the MDT (MSS-G) representing the same 18-year integration period has been calculated. In summary, the following key findings and results are highlighted:

1. New knowledge of the shape and spatial pattern of the MDT is derived at a spatial resolution of around 100 km and with an accuracy of around 4–5 cm which is superior to previous existing MDTs for this region.
2. Combined with the steric height estimated from hydrographic data, the pure barotropic contribution to the MDT shows distinct features in consistence with known deep barotropic circulations in the Norwegian and Greenland Seas.
3. The new GOCE-based MDT and surface geostrophic currents compare favorably with existing independent surface velocity calculations derived from combined altimeter data, in situ observations and gravity field models.
4. The transport estimates, both in the mean and seasonal signals, are also favoring the combined use of the GOCE-based surface geostrophic current and hydrographic data.

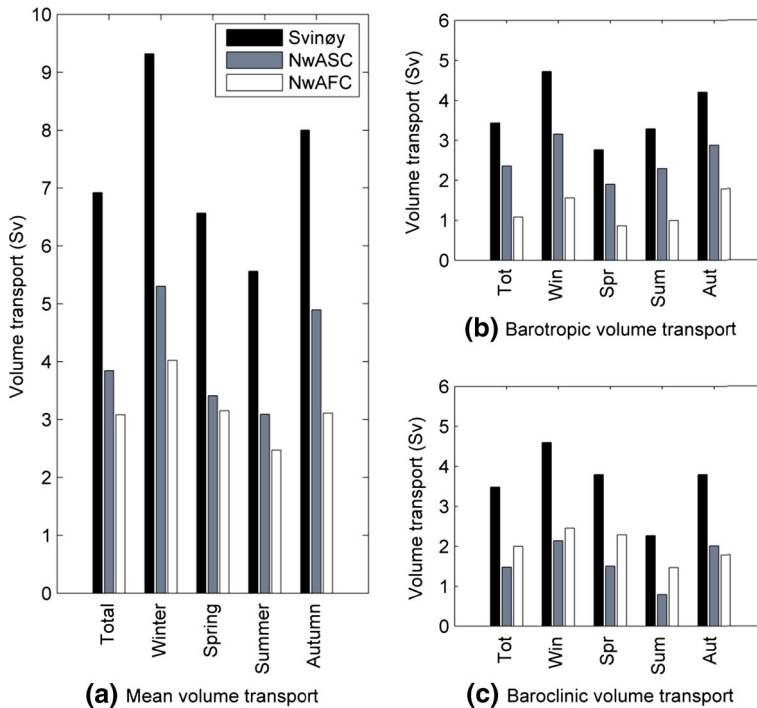


**Fig. 10** Mean annual and mean seasonal total volume transport estimates (a), the respective barotropic components (b) and baroclinic components (c) for the Svinøy section including the NwASC and the NwAFC for the period 1993–2010 based on combined use of GOCE, altimetry and in situ hydrography data. The grayscale legend is shown in (a)

5. New understanding of the relationship between the MDT, the mean surface geostrophic current and the magnitude of the mean ocean volume transport has been derived for the seasonal variability with regard to the inflow of Atlantic Water to the Norwegian Sea at the Svinøy section.
6. The NwASC contains approximately 60 % of the total volume flux across the Svinøy section with a distinct transport maximum in winter (Dec–Jan) and a minimum in summer (Jun–Aug). This transport is moreover dominated by the barotropic component.
7. These data and findings are also excellent for assessment and validation of model-based retrieval of the MDT, the surface geostrophic current and the volume transport across selected sections and straits.

Overall, the findings add new insight into the ocean circulation and transport between the northeast Atlantic Ocean and the Arctic Ocean. They are also considered to be highly valuable for further studies of the regional sea-level change in the Nordic Seas and the Arctic Ocean, notable via the contribution of steric height and changes in the volume transport. Consistent use of the GOCE data for assimilation as suggested by Haines et al. (2011) might also become feasible in near future.

Moreover, as gravity measurements provide an integrated view of the mass variations, their interpretation in terms of mass transport is inherently multidisciplinary. Satellite

gravimetry (such as combined GRACE and GOCE) is thus a vital component of a multi-sensor Earth-observing system, which complements and relates observations of different Earth system constituents in a common and consistent global framework (Panet et al. 2012). Being closely related to changes in sea level, ocean transports, glaciers and ice caps, future mass change observations from satellites (at a 100 km scale not resolved by GRACE today) have the potential to significantly advance the ability to monitor seasonal-to annual-to decadal variability in ocean mass transport.

**Acknowledgments** The work presented in this paper has partly been supported by European Union 7th Framework Program through the MONARCH-A Collaborative Project, FP7-Space-2009-1 contract no. 242446. In addition, it has been supported by the Research Council of Norway funded projects Number 200408 (SATICE) and number 212020 (GOCE MDT) and the (ESA/NRS) PRODEX project IGOCE, contract number 90377. The study was also partly funded by the Centre for Climate Dynamics at the Bjerknes Centre.

**Open Access** This article is distributed under the terms of the Creative Commons Attribution License which permits any use, distribution, and reproduction in any medium, provided the original author(s) and the source are credited.

## References

- AMAP (1998) AMAP assessment report: Arctic pollution issues. Arctic Monitoring and Assessment Programme (AMAP), Oslo, Norway, 859 pp
- Andersen OB, Knudsen P (2009) The DNSC08 mean sea surface and mean dynamic topography. *J Geophys Res* 114:C11. doi:[10.1029/2008JC005179](https://doi.org/10.1029/2008JC005179)
- Berx B, Hansen B, Østerhus S, Larsen KM, Sherwin T, Jochumsen K (2013) Combining in situ measurements and altimetry to estimate volume, heat and salt transport variability through the Faroe Shetland Channel. *Ocean Sci* 9. doi:[10.5194/os-9-639-2013](https://doi.org/10.5194/os-9-639-2013)
- Bingham RJ, Knudsen P, Andersen O, Pail R (2011) An initial estimate of the North Atlantic steady-state geostrophic circulation from GOCE. *Geophys Res Lett* 38:L01606. doi:[10.1029/2010GL045633](https://doi.org/10.1029/2010GL045633)
- Bleck Rainer (2002) An oceanic general circulation model framed in hybrid isopycnic-Cartesian coordinates. *Ocean Model* 4(1):55–88
- Bruinsma SL, Marty JC, Balmino G, Biancale R, Förste C, Abrikosov O and Neumayer H (2010) GOCE gravity field recovery by means of the direct numerical method, presented at the ESA Living Planet Symposium, 27th June–2nd July 2010, Bergen, Norway; See also: [earth.esa.int/GOCE](http://earth.esa.int/GOCE)
- Bruinsma SL, Förste C, Abrikosov O, Marty J-C, Rio M-H, Mulet S, Bonvalot S (2013) The new ESA satellite-only gravity field model via the direct approach. *Geophys Res Lett* 40:1–6. doi:[10.1002/grl.50716](https://doi.org/10.1002/grl.50716)
- Cazenave et al (2009) Sea level budget over 2003–2008: a re-evaluation from GRACE space gravimetry, satellite altimetry and Argo. *Global Planet Change* 65(1–2):83–88
- Cheng YO, Andersen and Knudsen P (2013) Evaluation of gridded and along-track altimetric data in the Arctic Ocean for climate research, submitted to *Marine Geodesy*
- Förste C, Bruinsma S, Shako R, Marty JC, Flechtner F, Abrikosov O, Dahle C, Lemoine, JM, Neumayer KH, Biancale R, Barthelmes F, König R, Balmino G (2011) EIGEN-6—A new combined global gravity field model including GOCE data from the collaboration of GFZPotsdam and GRGS-Toulouse; *Geophysical Research Abstracts*, vol. 13, EGU2011-3242-2, EGU General Assembly
- Fu L–L, Cheng B, Qiu B (2001) 25-day period large-scale oscillations in the Argentine Basin revealed by the TOPEX/POSEIDON altimeter. *J Phys Oceanogr* 31:506–517
- Furevik T, Nilsen JEØ (2005) Large-scale atmospheric circulation variability and its impacts on the Nordic Seas ocean climate—a review. In: *The Nordic Seas: an integrated perspective*. AGU Geophysical Monograph Series, vol 158. pp 105–136
- Gill AE, Niiler PP (1973) The theory of seasonal variability in the ocean. *Deep Sea Res* 20:141–177
- Haines K, Johannessen JA, Knudsen P, Lea D, Rio MH, Bertino L, Davidson F, Hernandez F (2011) An ocean modelling and assimilation guide to using GOCE geoid products. *Ocean Sci* 7(1):151–164
- Hansen B, Hatun H, Kristiansen R, Olsen SM, Østerhus S (2010) Stability and forcing of the Iceland-Faroe inflow of water, heat, and salt to the Arctic. *Ocean Sci* 6:1013–1026

- Hawkins E, Sutton R (2008) *Geophys Res Lett* 35:L11603. doi:[10.1029/2008GL034059](https://doi.org/10.1029/2008GL034059)
- Helland-Hansen B, Nansen F (1909) The Norwegian Sea: its physical oceanography based upon the Norwegian Researches 1900–1904, Report on Norwegian Fishery and Marine Investigation, vol. II. The Royal Department of Trade, Navigation and Industries, Mallingske, Kristiania, pp 390
- Henry O, Prandi P, Llovel W, Cazenave A, Jevrejeva S, Stammer D, Meyssignac B, Koldunov N (2012) Tide gauge-based sea level variations since 1950 along the Norwegian and Russian coasts of the Arctic Ocean: contribution of the steric and mass components. *J Geophys Res* 117(C6):C06 023. doi:[10.1029/2011JC007706](https://doi.org/10.1029/2011JC007706)
- Johannessen JA, Balmino G, Le Provost C, Rummel R, Sabadini R, Sünkel H, Tscherning CC, Visser P, Woodworth P, Hughes CW, LeGrand P, Sneeuw N, Perosanz F, Aguirre-Martinez M, Rebhan H, Drinkwater M (2003) The European gravity field and steady-state ocean circulation explorer satellite mission: impact in Geophysics. *Surv Geophys* 24:339–386
- Knudsen P, Bingham R, Andersen O, Rio Marie-Helene (2011) A global mean dynamic topography and ocean circulation estimation using a preliminary GOCE gravity model. *J Geodesy*. doi:[10.1007/s00190-011-0485-8](https://doi.org/10.1007/s00190-011-0485-8)
- Koldunov NV, Serra N, Kohl A, Stammer D, Henry O, Prandi P, Cazenave A, Knudsen P, Andersen OB, Gao Y, Johannessen JA (2013) Arctic Ocean Sea Surface Height variability during the last 40 years, *to be submitted to JGR*
- Koop R, Gruber T, Rummel R (2007) The status of the GOCE highlevel processing facility (HPF). In: Proceedings of the 3rd GOCE User Workshop, pp 199–204, European Space Research Institute, European Space Agency, Frascati, Italy
- Kwok R, Morison J (2011) Dynamic topography of the ice-covered Arctic Ocean from ICESat. *Geophys Res Lett* 38(2):L02 501. doi:[10.1029/2010GL046063](https://doi.org/10.1029/2010GL046063)
- Maximenko N, Niiler P, Rio M-H, Melnichenko O, Centurioni L, Chambers D, Zlotnicki V, Galperin B (2009) Mean dynamic topography of the ocean derived from satellite and drifting buoy data using three different techniques. *J Atmos Ocean Tech* 26(9):1910–1919
- McPhee MG (2013) Intensification of geostrophic currents in the Canada Basin, Arctic Ocean. *J Climate* 26. doi:[10.1175/JCLI-D-12-00289.1](https://doi.org/10.1175/JCLI-D-12-00289.1)
- Morison J, Kwok R, Peralta-Ferriz C, Alkire M, Rigor I, Andersen R, Steele M (2012) Changing Arctic Ocean freshwater pathways. *Nature* 481(7379):66–70. doi:[10.1038/nature10705](https://doi.org/10.1038/nature10705)
- Mork KA, Skagseth Ø (2005) Annual sea surface height variability in the Nordic Seas, in The Nordic Seas: An Integrated Perspective, *Geophys Monogr Ser*, vol. 158, edited by H. Drange et al. pp. 51–64, AGU, Washington, DC
- Mork KA, Skagseth Ø (2010) A quantitative description of the Norwegian Atlantic current by combining altimetry and hydrography. *Ocean Sci* 6:901–911. doi:[10.5194/os-6-901-2010](https://doi.org/10.5194/os-6-901-2010)
- Nilsen JEØ, Hatun H, Mork KA and Valdimarsson H (2008) The NISE Data Set. *Technical Report* 08-01, Faroese Fisheries Laboratory, Box 3051, Torshavn, Faroe Islands
- Nilsen JEØ, Falck E (2006) Variation of mixed layer properties in the Norwegian Sea for the period 1948–1999. *Prog Oceanogr* 70:58–90. doi:[10.1016/j.pocean.2006.03.014](https://doi.org/10.1016/j.pocean.2006.03.014)
- Nilsen JEØ, Nilsen F (2007) The Atlantic water flow along the Vøring plateau: detecting frontal structures in oceanic station time series. *Deep Sea Res Part 1* 54(3):297–319. doi:[10.1016/j.dsv.2006.12.012](https://doi.org/10.1016/j.dsv.2006.12.012)
- Nøst OA, Isachsen PE (2003) The large-scale time-mean ocean circulation in the Nordic seas and Arctic Ocean estimated from simplified dynamics. *J Mar Res* 61:175–210
- Orvik KA, Skagseth Ø (2003) Monitoring the Norwegian Atlantic slope current using a single moored current meter. *Cont Shelf Res* 23:159–176
- Orvik KA, Skagseth Ø (2005) Heat flux variations in the eastern Norwegian Atlantic current toward the Arctic from moored instruments, 1995–2005. *Geophys Res Lett* 32:L14610. doi:[10.1029/2005GL023487](https://doi.org/10.1029/2005GL023487)
- Orvik KA, Skagseth Ø, Mork M (2001) Atlantic inflow to the Nordic Seas: current structure and volume fluxes from moored current meters, VM-ADCP and SeaSoar-CTD observations, 1995–1999. *Deep-Sea Res I*:48. doi:[10.1016/S0967-0637\(00\)00038-8](https://doi.org/10.1016/S0967-0637(00)00038-8)
- Østerhus S, Turrrell WR, Jónsson S, Hansen B (2005) Measured volume, heat, and salt fluxes from the Atlantic to the Arctic Mediterranean. *Geophys Res Lett* 32:L07603. doi:[10.1029/2004GL022188](https://doi.org/10.1029/2004GL022188)
- Pail R, Bruinsma S, Migliaccio F, Foerste C, Goiginger H, Schuh W-D, Hoek E, Reguzzoni M, Brockmann JM, Abrikosov O, Veicherts M, Fecher T, Mayrhofer R, Krasbutter I, Sanso F, Tscherning CC (2011) First GOCE gravity field models derived by three different approaches. *J Geodesy* 85(11):819–843
- Panet I, Flury J, Biancale R, Gruber T, Johannessen JA, van den Broeke MR, van Dam P, Gegout T, Hughes CW, Ramillien G, Sasgen I, Seoane L, Thomas M (2012) Earth system mass transport mission (e.motion): a concept for future earth gravity field measurements from space. *Surv Geophys*. doi:[10.1007/s1072-012-9209-8](https://doi.org/10.1007/s1072-012-9209-8)

- Prandi P, Ablain M, Cazenave A, Picot N (2012) Sea level variability in the Arctic Ocean observed by satellite altimetry. *Ocean Sci Discuss* 9(4):2375–2401. doi:[10.5194/osd-9-2375-2012](https://doi.org/10.5194/osd-9-2375-2012)
- Rio MH, Guinehut S, Larnicol G (2011) New CNES-CLS09 global mean dynamic topography computed from the combination of GRACE data, altimetry, and in situ measurements. *J Geophys Res* 116:C07018. doi:[10.1029/2010JC006505](https://doi.org/10.1029/2010JC006505)
- Rosby T, Ozhigin V, Ivshin V, Bacon S (2009) An isopycnal view of the Nordic Seas hydrography with focus on properties of the Lofoten Basin. *Deep Sea Res Part 1* 56:1955–1971. doi:[10.1016/j.dsr.2009.07.005](https://doi.org/10.1016/j.dsr.2009.07.005)
- Sakov P, Counillon F, Bertino L, Lisæter KA, Oke PR, Korablev A (2012) TOPAZ4: an ocean-sea ice data assimilation system for the North Atlantic and Arctic. *Ocean Sci* 8:633–656. doi:[10.5194/os-8-633-2012](https://doi.org/10.5194/os-8-633-2012)
- Sandø AB, Nilsen JEØ, Eldevik T, Bentsen M (2012) Mechanisms for variable North Atlantic–Nordic seas exchanges. *J Geophys Res* 117:C12006. doi:[10.1029/2012JC008177](https://doi.org/10.1029/2012JC008177)
- Serra NRH, Käse A, Stammer Köhl D, Quadfasel D (2010) On the low-frequency phase relation between the Denmark Strait and the Faroe-Bank Channel overflows. *Tellus* 62:530–550. doi:[10.1111/j.1600-0870.2010.00445.x](https://doi.org/10.1111/j.1600-0870.2010.00445.x)
- Shum CK, Hans-Peter Plag, Jens Schröter, Victor Zlotnicki, Peter Bender, Alexander Braun, Anny Cazenave, Don Chamber, Jianbin Duan, William Emery, Georgia Fotopoulos, Viktor Gouretski, Richard Gross, Thomas Gruber, Junyi Guo, Guoqi Han, Chris Hughes, Masayoshi Ishii, Steven Jayne, Johnny A. Johannessen, Per Knudsen, Chung-Yen Kuo, Eric Leuliette, Sydney Levitus, Nikolai Maximenko, Laury Miller, James Morison, Harunur Rashid, John Ries, Markus Rothacher, Reiner Rummel, Kazuo Shibuya, Michael Sideris, Y. Tony Song, Detlef Stammer, Maik Thomas, Josh Willis, Philip Woodworth (2010) Geodetic observations of the ocean surface topography, geoid, currents and changes in ocean mass and volume, Plenary Session Paper, OceanObs09, Venice Italy, 21–25 Sept. 2009, *ESA Publication WPP 306*, doi: [10.5270/OceanObs09](https://doi.org/10.5270/OceanObs09)
- Siegmund F, Johannessen JA, Drange H, Mork KA, Korablev A (2007) Steric height variability in the Nordic Seas. *J Geophys Res* 112:C12010. doi:[10.1029/2007JC004221](https://doi.org/10.1029/2007JC004221)
- Skagseth Ø, Furevik T, Ingvaldsen R, Loeng H, Mork KA, Orvik KA, Ozhigin V (2008) Volume and Heat Transports to the Arctic Ocean via the Norwegian and Barents Seas. In: Dickson (ed) *Arctic-Subarctic Ocean Fluxes (ASOF): Defining the Role of the Northern Seas in Climate*. Springer, Berlin, pp 45–64
- Søiland H, Prater MD, Rosby T (2008) Rigid topographic control of currents in the Nordic Seas. *Geophys Res Lett* 35:L18607. doi:[10.1029/2008GL034846](https://doi.org/10.1029/2008GL034846)
- Stammer D (1997) Steric and wind-induced changes in TOPEX/POSEIDON large-scale sea surface topography observations. *J Geophys Res*. doi:[10.1029/97JC021009](https://doi.org/10.1029/97JC021009)
- Steele M, Ermold W (2007) Steric sea level change in the northern seas. *J Climate* 20. doi:[10.1175/JCLI4022.1](https://doi.org/10.1175/JCLI4022.1)
- Tomczak M, Godfrey JS (2003) *Regional Oceanography: An Introduction*, 2nd edn. Daya Publishing House, New Delhi